ELSEVIER

NeuroImage

www.elsevier.com/locate/ynimg
NeuroImage 40 (2008) 19–25

Brain white matter tracts degeneration in Friedreich ataxia. An in vivo MRI study using tract-based spatial statistics and voxel-based morphometry

Riccardo Della Nave,[a] Andrea Ginestroni,[a] Carlo Tessa,[b] Elena Salvatore,[c] Ilaria Bartolomei,[d] Fabrizio Salvi,[d] Maria Teresa Dotti,[e] Giuseppe De Michele,[c] Silvia Piacentini,[f] and Mario Mascalchi[a,*]

[a]*Radiodiagnostic Section, Department of Clinical Physiopathology, University of Florence, Florence, Viale Morgagni 85, 50134 Florence, Italy*
[b]*Radiology Unit, Versilia Hospital, Camaiore (Lucca), Italy*
[c]*Department of Neurological Sciences, University of Naples Federico II, Naples, Italy*
[d]*Department of Neurology, Bellaria Hospital, University of Bologna, Bologna, Italy*
[e]*Department of Neurological and Behavioural Sciences, University of Siena, Siena, Italy*
[f]*Department of Neurological and Psychiatric Sciences, University of Florence, Florence, Italy*

Received 8 August 2007; revised 17 November 2007; accepted 22 November 2007
Available online 14 December 2007

Background and purpose: **Neuropathological examination in Friedreich ataxia (FRDA) reveals neuronal loss in the gray matter (GM) nuclei and degeneration of the white matter (WM) tracts in the spinal cord, brainstem and cerebellum, while the cerebral hemispheres are substantially spared. Tract-based spatial statistics (TBSS) enables an unbiased whole-brain quantitative analysis of the fractional anisotropy (FA) and mean diffusivity (MD) of the brain WM tracts in vivo.**

Patients and methods: **We assessed with TBSS 14 patients with genetically confirmed FRDA and 14 age- and sex-matched healthy controls who were also examined with voxel-based morphometry (VBM) to assess regional atrophy of the GM and WM.**

Results: **TBSS revealed decreased FA in the inferior and superior cerebellar peduncles and the corticospinal tracts in the medullary pyramis, in WM tracts of the right cerebellar hemisphere and in the right occipito-frontal and inferior longitudinal fasciculi. Increased MD was observed in the superior cerebellar peduncles, deep cerebellar WM, posterior limbs of the internal capsule and retrolenticular area, bilaterally, and in the WM underlying the left central sulcus. Decreased FA in the left superior cerebellar peduncle correlated with clinical severity. VBM showed small symmetric areas of loss of bulk of the peridentate WM which also correlated with clinical severity.**

Conclusions: **TBSS enables in vivo demonstration of degeneration of the brainstem and cerebellar WM tracts which neuropathological examination indicates to be specifically affected in FRDA. TBSS complements VBM and might be a more sensitive tool to detect WM structural changes in degenerative diseases of the CNS.**

Keywords: DWI; Tract-based spatial statistics; Gait disorders/ataxia; Friedreich ataxia

Introduction

Friedreich ataxia (FRDA) is the most common inherited ataxia and in most cases is due to a GAA repeat expansion in a gene on chromosome 9q13 coding for a mitochondrial protein named frataxin (Klockgether, 2000). Neuropathological studies show that FRDA is characterized by neuronal loss and WM tracts degeneration in the spinal cord, brainstem and cerebellum (Lowe et al., 1997). MRI studies in FRDA patients pointed out atrophy of the cervical spinal cord and dorsal medulla, of the GM in the rostral vermis and infero-medial portions of the cerebellar hemispheres and of the WM in the peridentate regions (Della Nave et al., 2007; Schols et al., 1997; Wullner et al., 1993; Huang et al., 1993). No signal change, notably with a tract distribution, was reported in the brain of patients with FRDA, but using a T2*-weighted sequence Waldvogel et al. (1999) reported abnormally increased T2* relaxation rate assumed to reflect increased iron content in the dentate nuclei of the cerebellum. Conversely, the atrophy of the spinal cord is combined with symmetric hyperintensity in proton density and T2-weighted images of the WM tracts in the lateral and posterior columns of cervical spinal cord reflecting wallerian

* Corresponding author.
E-mail address: m.mascalchi@dfc.unifi.it (M. Mascalchi).
Available online on ScienceDirect (www.sciencedirect.com).

1053-8119/$ - see front matter © 2007 Elsevier Inc. All rights reserved.
doi:10.1016/j.neuroimage.2007.11.050

degeneration in the cuneatus, gracilis and spinocerebellar tracts (Mascalchi et al., 1995).

In last years the capability of diffusion tensor MR images (DTI) to demonstrate the WM tracts has found increasing application for the structural evaluation of the normal and abnormal brain (Mori and Zhang, 2006). Recently, a voxel-wise analysis of multi-subject diffusion tensor data named tract-based spatial statistics (TBSS) was developed (Smith et al., 2006, 2007).

We hypothesized that TBSS could demonstrate in vivo the degenerating WM tracts in the brain of patients with genetically proven FRDA. Moreover we compared the sensitivity of TBSS in revealing structural damage of the brain WM tracts with that of voxel based morphometry (VBM) in detecting brain GM and WM atrophy in the same patients.

Patients and methods

Between March 2006 and April 2007 fourteen consecutive outpatients (9 women, 5 men, mean age 31±9 years) with genetically proven FRDA regularly followed at the ambulatories for ataxic diseases of the Neurological Department of the University of Florence, Siena and Bologna gave their informed consent to participate in this prospective study which was approved by the Ethical Committee of the University of Florence.

Molecular diagnostic methods were previously reported (Bidichandani et al., 1998) and the cut-off number of triplets repeats expansion qualifying for diagnosis was 100 GAA on both alleles for FRDA.

On the day of the MR examination, the same neurologist blind to the results of MR defined the patient's disease duration and computed her or his scores on the Inherited Ataxia Clinical Rating Scale (IACRS) (Filla et al., 1990). The IACRS is a 0–46 semi-quantitative scale with 46 corresponding to maximal clinical deficit which evaluates signs and symptoms related to ataxia, pyramidal tract dysfunction and impaired vibration or position sense. Mean disease duration was 17 years (range 5–31) and mean IACRS score was 27 (range 9–36).

Fourteen healthy volunteers (5 women and 9 men; mean age 31±6 years) without personal of familial history of neurological disease served as controls.

MR examination

Patients and controls underwent MR imaging examination in a single center on a 1.5 T system (Philips Intera, Best The Netherland) with 33 mT/m maximum gradient strength and SENSE coil technology. After scout and axial proton density and T2-weighted images (TR=2000 ms, TE 20/120 ms, FOV=256 mm, matrix size 256×288, 20 slices, slice thickness=5 mm, NEX=2), axial DTI with single-shot echo planar imaging sequence (TR=9394 ms, TE=89 ms, FOV=256 mm, matrix size=128×128, 50 slices, slice thickness=3 mm, no gap, NEX=3) was also acquired on axial plane for TBSS. Diffusion sensitizing gradients were applied along 15 non-collinear directions using b value of 0 (b_0 image) and 1000 s/mm^2. Maps of fractional anisotropy (FA) and mean diffusivity (MD) were calculated from the DTI after both automatic segmentation of the brain from the non-brain tissue and eddy currents correction by means of FDT 1.0 (FMRIB's Diffusion Toolbox 1.0 (Behrens et al., 2003) part of FSL 3.3; FMRIB Image Analysis Group, Oxford, UK) (Smith et al., 2004).

To assess regional atrophy, patients and controls were also examined with axial 3D T1-weighted turbo gradient echo [repetition time (TR)=25 ms, echo time (TE)=4.6 ms, flip angle=30°, field of view (FOV)=256 mm, matrix size=256×256, 160 contiguous slices, slice thickness=1 mm] images for VBM.

Data processing

Image data processing was performed on a PC running FMRIB Software Library (FSL) 3.3 package (FMRIB Image Analysis Group, Oxford, UK) (Smith et al., 2004) and the statistical parametric mapping 2 (SPM2) software (Wellcome Department of Cognitive Neurology, London, UK).

Preliminarily proton density and T2-weighted images were subjectively evaluated for focal abnormalities which can influence TBSS results. Moreover DTI and T1-weighted images were evaluated for motion artifacts before entering image processing.

TBSS analysis was performed using TBSS 1.0 tool part of the FSL 3.3 and is described in detail elsewhere (Smith et al., 2006, 2007). In brief, TBSS implies a four-step approach: identification of a common registration target and alignment of all subject's FA images to this target, creation of the mean of all aligned FA images and of a skeletonized mean FA image which is thresholded, projection of each subject's FA image onto the skeleton, voxel-wise statistic analysis across subject on the skeleton-space FA data. Using the same nonlinear registration, skeleton and skeleton projection vectors derived from the FA analysis, MD data were projected onto the skeleton before voxel-wise statistic analysis across subject (Smith et al., 2007).

The methodology of VBM closely followed that previously reported (Good et al., 2001) and included six steps: reorientation according to the antero-posterior commissure line, template creation to improve brains segmentation, normalization, segmentation in 3 classes of tissue (GM, WM and CSF), smoothing with a 8 mm full width half-maximum Gaussian kernel, and voxel-wise between groups statistical analysis.

Statistical methods

TBSS

Group comparison for FA and MD data was performed using permutation-based nonparametric inference on cluster size (Nichols and Holmes, 2002) and Randomise software part of FSL 3.3. A restrictive statistical thresholds was used (cluster-based thresholding $t>3$, $p<0.05$, corrected for multiple comparisons) (Smith et al., 2006).

In addition, only in FRDA patients we correlated FA and MD with each patient's IACRS score using the same software and permutation-based nonparametric inference on cluster size ($t>3$, $p<0.05$ corrected) (Smith et al., 2006).

Identification of the abnormal WM tracts revealed by TBSS was based on the Atlas made by Wakana et al. (2004) and the Testut and Latarjet's (1971) textbook of anatomy.

VBM

Statistical analysis of the MR data was based on the general linear model and the theory of Gaussian random fields. A voxel-wise comparison of spatially normalized T1-weighted images was made using SPM2. Group comparisons were performed by means of analysis of covariance (ANCOVA) using the total volume of each segmented image (GM volume for GM analysis, WM volume

for WM analysis) as confounding covariate. Age and gender were included as covariates of no interest to exclude possible effects of these variables on regional GM or WM volumes (Good et al., 2001).

Voxel-level analysis with a significance threshold set at p-value <0.05 corrected for multiple comparisons across the whole brain [family wise error (FWE) correction] was applied to the resulting t-statistic maps of GM and WM.

To correlate extent of volume loss with severity of the clinical deficit, the significant areas at group analysis were saved and applied as regions of interest (ROI) on the maps of local average volume of each patient. Extracted local average volumes for each region of decreased bulk were finally correlated with the IACRS scores by means of the Spearman rank correlation test ($p<0.05$).

Results

No signal changes in PD- and T2-weighted images were seen in the brain of 13 FRDA patients and all controls. In one FRDA patient a small cavernous angioma was present in the right peritrigonal white matter. No motion artifacts in DTI and T1-weighted images were observed in patients and controls.

TBSS group comparison revealed in FRDA patients a nearly symmetric decrease of FA (Fig. 1) in many WM tracts of the brainstem and cerebellum including the inferior and superior cerebellar peduncles, the corticospinal tract at the level of the medulla (pyramis) and in WM tracts of the right cerebellar hemisphere. In the cerebral hemispheres, decrease of the FA was observed only in the right occipitofrontal fasciculus and the inferior longitudinal fasciculus.

TBSS group comparison revealed in FRDA patients an increase of MD (Fig. 2) in deep cerebellar WM, the superior cerebellar peduncles, posterior limbs of the internal capsule and retro-lenticular area, bilaterally. An area of increased MD was also present in the WM underlying the left central sulcus.

The coordinates of the clusters of decreased FA and increased MD in FRDA patients vs. controls are detailed in Table 1.

The severity of the clinical deficit as assessed with the IACRS score correlated with the decreased FA in the left superior cerebellar peduncle (Fig. 3). No correlation between the IACRS score and areas of increased MD was present.

VBM showed two small areas of decreased volume in the peridentate WM ($x=5$, $y=-60$, $z=-33$, $t=7.06$, $p_{fwe}=0.014$; $x=-6$, $y=-56$, $z=-33$, $t=6.64$, $p_{fwe}=0.030$) (Fig. 4), whereas no atrophy of the GM was observed. The decreased cerebellar WM volume correlated with the severity of the clinical deficit ($R=-0.55$; $p=0.04$).

Discussion

VBM and TBSS are automated methods which explore the whole-brain with an intrinsically strong statistical power and without any a priori hypothesis. In particular, TBSS enables investigation of WM tracts without the limitations caused by alignment inaccuracies and by uncertainty about smoothing extent typical of other voxel-wise methods of analysis of FA and MD data (Smith et al., 2006, 2007).

The combination of molecular genetic diagnosis with VBM or TBSS offers the possibility to perform an in vivo assessment of the structural changes associated with inherited ataxias (Brenneis et al., 2003; Lasek et al., 2006; Lukas et al., 2006; Della Nave et al.,

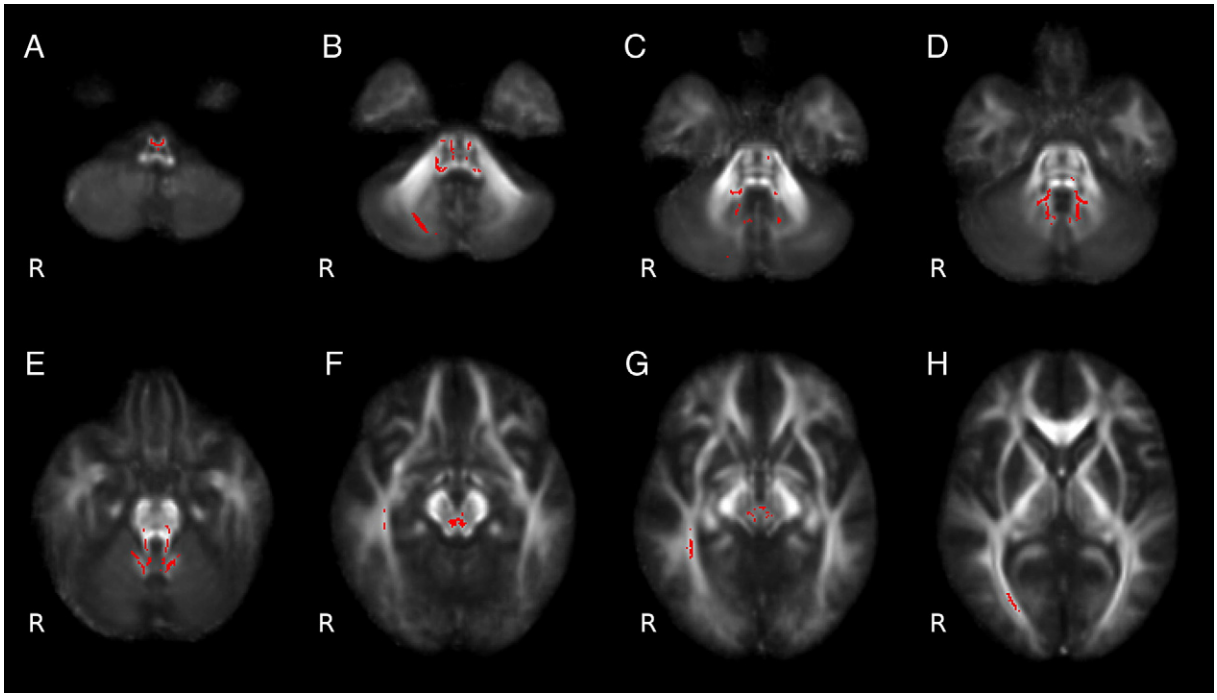

Fig. 1. (A–H) TBSS analysis of FA maps. Maps of the t-value ($t>3$ with $p<0.05$ corrected for multiple comparisons) showing in red the clusters of significantly reduced FA in WM tracts in FRDA patients as compared to controls: corticospinal tracts at the medullary pyramids (A); inferior cerebellar peduncles and right cerebellar hemisphere WM (B); superior cerebellar peduncles (C–E); decussation of the superior cerebellar peduncles in the midbrain (F and G) and right inferior fronto-occipital and inferior longitudinal fasciculus (F–H).

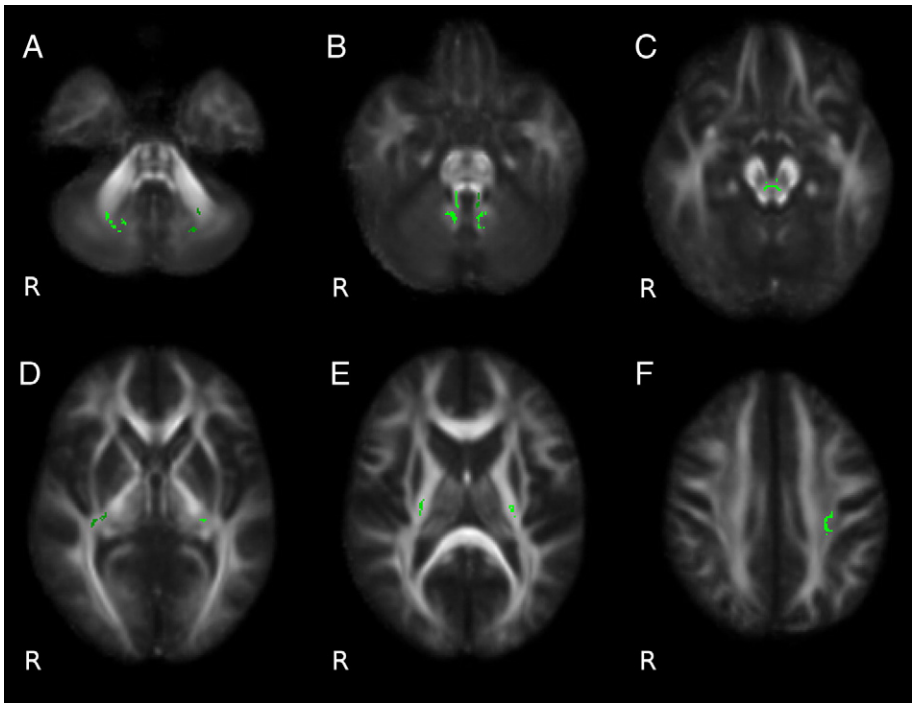

Fig. 2. (A–F) TBSS analysis of MD maps. Maps of the *t*-value ($t>3$ with $p<0.05$ corrected for multiple comparisons) showing in green the clusters of significantly increased MD in WM tracts in FRDA patients as compared to controls: deep cerebellar WM, bilaterally (A), superior cerebellar peduncles (B); decussation of the superior cerebellar peduncles in the midbrain (C) retrolenticular area, bilaterally (D); posterior limb of the internal capsule, bilaterally (E). An area of increased MD was also present in the WM underlying the left central sulcus (F).

2007). These are rare conditions whose neuropathological examination is influenced by several limitations including the usually small number of available cases, the technical (fixation artifacts etc.) and sample (a whole-brain neuropathological examination is rarely performed) bias and the coexistence of agonal changes. In the case of FRDA these difficulties are

Table 1
Coordinates of the center of mass (Montreal Neurological Institute) of decreased FA and increased MD in FRDA patients vs. healthy controls

Cluster size	*p*	MNI coordinates			Areas
		x	*y*	*z*	
FA					
498	0.001	0	−31	−51	Corticospinal tract (medulla)
232	0.006	11	−41	−40	Inferior cerebellar peduncles R
200	0.015	−8	−41	−41	Inferior cerebellar peduncles L
136	0.026	23	−73	−41	Cerebellar hemisphere R
402	0.003	9	−48	−30	Superior cerebellar peduncles R
316	0.004	−8	−50	−29	Superior cerebellar peduncles L
583	0.000	0	−26	−14	Superior cerebellar peduncles decussation
221	0.007	43	−36	−9	Inferior longitudinal fasciculus R
267	0.004	29	−3	3	Inferior fronto-occipital fasciculus R
MD					
248	0.001	26	−63	−41	Cerebellar hemisphere R
62	0.035	−23	−65	−38	Cerebellar hemisphere L
187	0.002	8	−47	−28	Superior cerebellar peduncles R
189	0.002	−5	−55	−25	Superior cerebellar peduncles L
154	0.003	1	−27	−16	Superior cerebellar peduncles decussation
62	0.035	−32	−25	−3	Retrolenticular part of the internal capsule L
62	0.035	34	−25	−1	Retrolenticular part of the internal capsule R
85	0.024	27	−19	8	Posterior limb of the internal capsule R
137	0.004	−27	−20	12	Posterior limb of the internal capsule L
156	0.003	−30	−28	40	Corticospinal tract L

R = right; L = left.

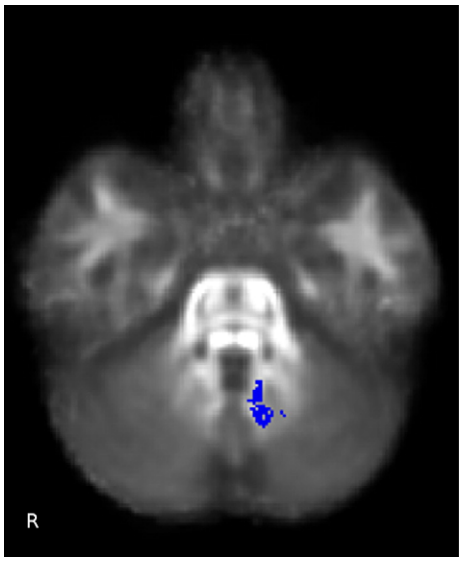

Fig. 3. TBSS results. Blue shows an area the left superior cerebellar peduncle where FA correlates negatively ($t>3$ with $p<0.05$ corrected for multiple comparisons) with the IACRS score in patients with FRDA.

accompanied by heterogeneity of the clinical presentation (Durr et al., 1996; Schols et al., 1997) which justifies some caution about the homogeneity of the cases which underwent neuropathological examination before availability of molecular genetic tests.

Neuropathological hallmark of FRDA is neuronal loss and shrinkage in the spinal ganglion cells and in the Clarke column of the spinal cord with degeneration of the gracilis and cuneatus tracts in the posterior columns and of the spinocerebellar tracts in the lateral columns of the spinal cord (Lowe et al., 1997; Lamarche et al., 1984). While secondary neuronal loss in the brainstem predominantly involves the accessory cuneate and gracile nuclei of the dorsal medulla, atrophy of the inferior cerebellar peduncles containing the spinocerebellar fibers directed to the vermian cortex is common. The cerebellar cortex and the inferior olives are spared, and the most striking feature in the cerebellum is a loss of neurons in the dentate nuclei with severe atrophy of the superior cerebellar peduncles containing most of the efferent fibers of the dentate which project to the frontal cortex directly or through the thalami (Lowe et al., 1997). The cerebellar white matter is diffusely gliotic and there is loss of the myelinated fibers in the hilum of the dentate nuclei (Lowe et al., 1997; Lamarche et al., 1984). Cell loss and astrocytosis occur in the vestibular and cochlear nuclei and in the superior olives. Most cases show degenerative changes in the corticospinal tracts at the level of the medulla oblongata and below, whereas pathological abnormalities in the supratentorial compartment are usually restricted to optic nerve and tract damage and to loss or shrinkage of the Betz and other pyramidal neurons of the motor cortex (Lowe et al., 1997; Rewcastle, 1991).

In our study TBSS analysis revealed multiple WM tract changes in the brainstem, cerebellum and cerebral hemispheres in patients with FRDA as compared to healthy controls confirming the greater sensitivity of DTI in the evaluation of WM tract pathology as compared to conventional proton density and T2-weighted MR imaging which in our series failed to show any brain signal change with a tract distribution.

However TBSS analysis of FA and MD maps yielded only partially overlapping results.

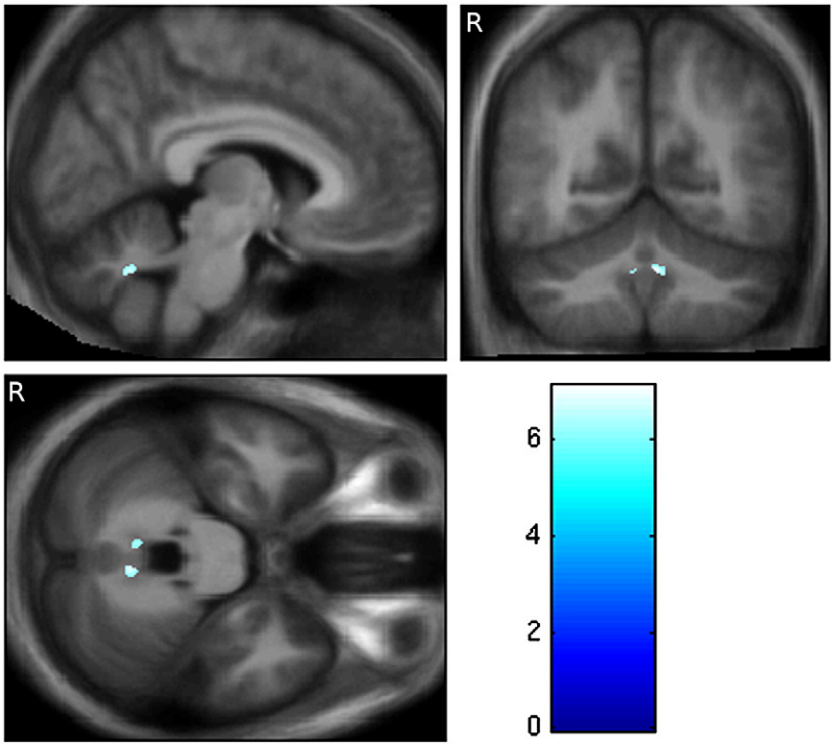

Fig. 4. VBM analysis. Maps of the t-value (voxel analysis at $p<0.05$ FWE corrected for multiple comparisons) superimposed on T1-weighted images showing in blue two small areas of decreased WM volume in the dentate regions in FRDA patients compared to healthy controls.

This confirms that FA and MD are not equivalent measurements (Pierpaoli et al., 2001; Cosottini et al., 2005) and justifies further investigations to explore their contribution in understanding pathophysiology of WM tracts in disease conditions.

In particular in our series only the superior cerebellar peduncles showed at the same time decreased FA and increased MD reflecting a presumably severe degeneration which was correlated in case of the left superior cerebellar peduncle with severity of neurological deficit. Interestingly, the superior cerebellar peduncles mainly contain efferent fibers from the dentate nuclei and the latter was found to show increased iron associated with neurodegeneration in FRDA (Waldvogel et al., 1999). Hence the symmetric severe damage of the WM tracts of the superior cerebellar peduncles well fits with the available neuropathological and MR imaging data.

Conversely, TBSS analysis revealed different areas of decreased FA and increased MD in FRDA patients as compared to healthy controls.

The symmetrically decreased FA in the inferior cerebellar peduncles and corticospinal tracts in the ventral medulla (pyramids) is expected based on the clinical and neurophysiological features of FRDA (Klockgether, 2000) and matches the available neuropathological descriptions (Lowe et al., 1997; Rewcastle, 1991).

In our series TBSS also showed decreased FA and increased MD in some WM tracts in the cerebellar hemispheres which can be expected based on the distribution of the neuropathological changes in FRDA.

Less obvious is the explanation of the decreased FA in the right inferior fronto-occipital fasciculus and inferior longitudinal fasciculus and of the increased MD in the posterior limbs of the internal capsule and retrolenticular area, bilaterally, and in the WM underlying the left central sulcus and of the increase of the MD in the posterior limbs of the internal capsule and retrolenticular area and in the WM underlying the L central sulcus.

We speculate that WM changes in the posterior limbs of the internal capsules and in the WM underlying the left central sulcus could reflect degeneration of the fibers belonging to the corticospinal tracts or spino-bulbo-thalamo-cortical pathway conducting the deep somatosensory and tactile sensation which are closely intermingled at these levels (Testut and Latarjet, 1971). On the other hand, the retrolenticular area, the inferior longitudinal fasciculus and inferior fronto-occipital fasciculus represent part of the visual pathway and visual association fibers, respectively (Testut and Latarjet, 1971). Hence these WM tract changes might correspond to degeneration associated with visual dysfunction which is clinically common in advanced FRDA (Klockgether, 2000) and is often demonstrated by neurophysiological studies in FRDA patients without visual complaints (Carroll et al., 1980). None of our patients complained of visual problems, but, unfortunately, they did not undergo neurophysiological examination at the time of the study.

Finally, we would like to comment on the asymmetry of some of the WM changes we observed. In our opinion this probably reflects a low statistical power since by decreasing the statistical threshold the WM alteration tended to become bilateral as expected in degenerative diseases of the CNS.

The capability of DTI to demonstrate degenerating WM tracts in the cerebellar peduncles with a disease characteristic distribution was recently reported by Taoka et al. (2007) in patients with spinocerebellar degenerative diseases different from FRDA. In particular they observed decrease of the FA in the superior, middle and inferior cerebellar peduncles in patients with dentatorubropallidoluysian atrophy, whereas decreased FA selectively involved the middle cerebellar peduncles in patients with multi-system atrophy, cerebellar type. Interestingly, no abnormalities of the FA in the cerebellar peduncles were observed in patients with late onset cerebellar cortical atrophy who typically exhibit sparing of the cerebellar peduncles at the neuropathological examination (Lowe et al., 1997). However they used a combined tractography and region of interest approach to measure the apparent diffusion coefficient and FA, which both involve an a priori knowledge bias.

Interestingly, in our small group of FRDA patients VBM demonstrated limited regional atrophy of the peridentate WM without any significant brainstem or cerebellar GM loss of bulk. Conversely, the latter and more extensive loss of peridentate WM was observed using VBM in a larger sample size of FRDA patients (Della Nave et al., 2007). This suggests that TBSS complements VBM and might be a statistically more powerful tool to detect structural WM changes as compared to VBM. While also the correlation between the reduced FA in the left superior cerebellar peduncle and the severity of the clinical deficit suggests a potential role of TBSS beside VBM in MRI evaluation of degenerative diseases of the CNS as FRDA, this requires further investigations in greater sample size and in other neurodegenerative diseases.

A technique to assess the size of major WM tracts from diffusion tensor data was recently proposed (Pagani et al., 2007) and two studies indicated that quantitative evaluation with DTI of the cervical spinal cord is now feasible (Valsasina et al., 2005; Agosta et al., 2007). Combination of these techniques with TBSS and VBM could further improve our understanding of WM tract pathophysiology in FRDA, but this was not investigated in the present study.

Acknowledgments

This study was supported in part by research grants of the Italian Ministry of Research to Professor Giuseppe De Michele (PRIN 2005) and to Professor Mario Mascalchi (PRIN 2007).

References

Agosta, F., Laganà, M., Valsasina, P., Dall'Occhio, L., Soriani, M.P., Judica, E., Filippi, M., 2007. Evidence for cervical cord tissue disorganisation with aging by diffusion tensor MRI. NeuroImage 36, 728–735.

Behrens, T.E., Woolrich, M.W., Jenkinson, M., Johansen-Berg, H., Nunes, R.G., Clare, S., Matthews, P.M., Brady, J.M., Smith, S.M., 2003. Characterization and propagation of uncertainty in diffusion-weighted MR imaging. Magn. Res. Med. 50, 1077–1088.

Bidichandani, S.I., Ashizawa, T., Patel, P.I., 1998. The GAA triplet-repeat expansion in Friedreich ataxia interferes with transcription and may be associated with an unusual DNA structure. Am. J. Hum. Genet. 62, 111–121.

Brenneis, C., Bösch, S.M., Schocke, M., Wenning, G.K., Poewe, W., 2003. Atrophy pattern in SCA2 determined by voxel-based morphometry. NeuroReport 14, 1799–1802.

Carroll, W.M., Kriss, A., Baraitser, M., Barrett, G., Halliday, A.M., 1980. The incidence and nature of visual pathway involvement in Friedreich's ataxia. A clinical and visual evoked potential study of 22 patients. Brain 103, 413–434.

Cosottini, M., Giannelli, M., Siciliano, G., Lazzarotti, G., Nichelassi, M.C., Del Corona, A., Bartolozzi, C., Murri, L., 2005. Diffusion-tensor MR imaging of corticospinal tract in amyotrophic lateral sclerosis and progressive muscular atrophy. Radiology 237, 258–264.

Della Nave, R., Ginestroni, A., Giannelli, M., Tessa, C., Salvatore, E., Salvi, F., Dotti, M.T., De Michele, G., Piacentini, S., Mascalchi, M., 2007. Brain structural damage in Friedreich ataxia. A MRI study using VBM. J. Neurol. Neurosurg. Psychiatry 79, 82–85.

Dürr, A., Cossee, M., Agid, Y., Campuzano, V., Mignard, C., Penet, C., Mandel, J.L., Brice, A., Koenig, M., 1996. Clinical and genetic abnormalities in patients with Friedreich's ataxia. N. Engl. J. Med. 335, 1169–1175.

Filla, A., DeMichele, G., Caruso, G., Marconi, R., Campanella, G., 1990. Genetic data and natural history of Friedreich's disease: a study of 80 Italian patients. J. Neurol. 237, 345–351.

Good, C.D., Johnsrude, I.S., Ashburner, J., Henson, R.N., Friston, K.J, Frackowiak, R.S., 2001. A voxel-based morphometric study of ageing in 465 normal adult human brains. NeuroImage 14, 21–36.

Huang, Y.P., Tuason, M.Y., Wu, T., Plaitakis, A., 1993. MRI and CT features of cerebellar degeneration. J. Formos. Med. Assoc. 92, 494–508.

Klockgether, T., 2000. Handbook of Ataxia Disorders. Marcel Dekker, New York.

Lamarche, J.B., Lemieux, B., Lieu, H.B., 1984. The neuropathology of "typical" Friedreich's ataxia in Quebec. Can. J. Neurol. Sci. 11, 592–600.

Lasek, K., Lencer, R., Gaser, C., Hagenah, J., Walter, U., Wolters, A., Kock, N., Steinlechner, S., Nagel, M., Zühlke, C., Nitschke, M.F., Brockmann, K., Klein, C., Rolfs, A., Binkofski, F., 2006. Morphological basis for the spectrum of clinical deficits in spinocerebellar ataxia 17 (SCA17). Brain 129, 341–2352.

Lowe, J., Lennox, G., Leigh, P.N., 1997. Disorders of movement and system degeneration, In: Graham, D.L., Lantos, P.L. (Eds.), 6th ed. Greenfield's Neuropathology, vol. 2. Arnold, London, UK, pp. 281–366.

Lukas, C., Schöls, L., Bellenberg, B., Rüb, U., Przuntek, H., Schmid, G., Köster, O., Suchan, B., 2006. Dissociation of grey and white matter reduction in spinocerebellar ataxia type 3 and type 6: a voxel-based morphometry study. Neurosci. Lett. 408, 230–235.

Mascalchi, M., Salvi, F., Piacentini, S., Bartolozzi, C., 1995. Friedreich 's ataxia: MR findings involving the cervical portion of the spinal cord. AJR Am. J. Roentgenol. 163, 187–191.

Mori, S., Zhang, J., 2006. Principles of diffusion tensor imaging and its applications to basic neuroscience research. Neuron 51, 527–539.

Nichols, T.E., Holmes, A.P., 2002. Nonparametric permutation tests for functional neuroimaging: a primer with examples. Hum. Brain Mapp. 15, 1–25.

Pagani, E., Horsfield, M.A., Rocca, M.A., Filippi, M., 2007. Assessing atrophy of the major white matter fiber bundles of the brain from DT MRI data. Magn. Res. Med. 58, 527–534.

Pierpaoli, C., Barnett, A., Pajjevic, S., Chen, R., Penix, L., Virta, A., Basser, P., 2001. Water diffusion changes in wallerian degeneration and their dependence on white matter architecture. NeuroImage 13, 1174–1185.

Rewcastle, N.B., 1991. Degenerative diseases of the central nervous system, In: Davis, R.L., Robertson, D.M. (Eds.), Textbook of Neuropathology, Second Edition. Williams and Wilkins, Baltimore, MD, pp. 904–906.

Schöls, L., Amoiridis, G., Przuntek, H., Frank, G., Epplen, J.T., Epplen, C., 1997. Friedreich's ataxia. Revision of the phenotype according to molecular genetics. Brain 120, 2131–2140.

Smith, S.M., Jenkinson, M., Woolrich, M.W., Beckmann, C.F., Behrens, T.E., Johansen-Berg, H., Bannister, P.R., De Luca, M., Drobnjak, I., Flitney, D.E., Niazy, R.K., Saunders, J., Vickers, J., Zhang, Y., De Stefano, N., Brady, J.M., Matthews, P.M., 2004. Advances in functional and structural MR image analysis and implementation as FSL. NeuroImage 23, 208–219.

Smith, S.M., Jenkinson, M., Johansen-Berg, H., Rueckert, D., Nichols, T.E., Mackay, C.E., Watkins, K.E., Ciccarelli, O., Cader, M.Z., Matthews, P.M., Behrens, T.E., 2006. Tract-based spatial statistics: voxelwise analysis of multi-subject diffusion data. NeuroImage 31, 1487–1505.

Smith, S.M., Johansen-Berg, H., Jenkinson, M., Rueckert, D., Nichols, T.E., Miller, K.L., Robson, M.D., Jones, D.K., Klein, J.C., Bartsc, A.J., Behrens, T.E., 2007. Acquisition and voxelwise analysis of multi-subject diffusion data with Tract-Based Spatial Statistics. Nature Protocols 3, 499–503.

Taoka, T., Kin, T., Nakagawa, H., Hirano, M., Sakamoto, M., Wada, T., Takayama, K., Wuttikul, C., Iwasaki, S., Ueno, S., Kichikawa, K., 2007. Diffusivity and diffusion anisotropy of cerebellar peduncles in cases of spinocerebellar degenerative disease. NeuroImage 37, 387–393.

Testut, L., Latarjet, 1971. Traité d'Anatomie Humaine, 9th Edition. G. Dion & C.ie, Paris.

Valsasina, P., Rocca, M.A., Agosta, F., Benedetti, B., Horsfield, M.A., Gallo, A., Rovaris, M., Comi, G., Filippi, M., 2005. Mean diffusivity and fractional anisotropy histogram analysis of the cervical spinal cord in MS patients. NeuroImage 26, 822–828.

Wakana, S., Jiang, H., Nagae-Poetscher, L.M., van Zijl, P.C., Mori, S., 2004. Fiber tract-based atlas of human white matter anatomy. Radiology 230, 77–87.

Waldvogel, D., van Gelderen, P., Hallet, M., 1999. Increased iron in the dentate nucleus of patients with Friedreich's ataxia. Ann. Neurol. 46, 123–125.

Wullner, U., Klockgether, T., Petersen, D., Naegele, T., Dichgans, J., 1993. Magnetic resonance imaging in hereditary and idiopathic ataxia. Neurology 43, 318–325.